Quaternary International 358 (2015) 12–20

Contents lists available at ScienceDirect

Quaternary International

journal homepage: www.elsevier.com/locate/quaint

Optical dating of young glacial sediments from the source area of the Urumqi River in Tianshan Mountians, northwestern China

XianJiao Ou [a, *], ZhongPing Lai [b, c, **], ShangZhe Zhou [d], Rong Chen [e], LanHua Zeng [a]

[a] School of Geography and Tourism, Jiaying University, Meizhou, Guangdong, 514015, China
[b] State Key Laboratory of Cryospheric Sciences, Cold and Arid Regions Environmental and Engineering Research Institute, Chinese Academy of Sciences, Lanzhou, 730000, China
[c] School of Earth Sciences, China University of Geosciences, Wuhan, 430074, China
[d] School of Geographical Science, South China Normal University, Guangzhou, 510631, China
[e] Nanjing Institute of Geography and Limnology, Chinese Academy of Sciences, Nanjing, 210008, China

A R T I C L E I N F O

Article history:
Available online 11 October 2014

Keywords:
OSL dating
Mountain glacier
Young glacial sediments
Residual dose
Urumqi River
Tianshan Mountains

A B S T R A C T

Incomplete bleaching, which will lead to overestimation of age, still remains one of the most significant problems in luminescence dating on glacial sediments. In order to test the bleachability of luminescence signals of mountain glacial sediments, nineteen young samples from different geomorphological positions and different sediment settings, in the source area of the Urumqi River in Tianshan Mountains, a key area of Quaternary glaciation study in China, were collected and dated using optically stimulated luminescence (OSL) dating methods. Equivalent dose (D_e) was determined by quartz SAR-SGC procedures. Results show that most of the samples suffer from varying degrees of overestimation. In general, glaciofluvial and lateral moraine till samples show relatively low residual doses (0–20.5 Gy); while subglacial tills, tills from terminal moraines, ground moraines and hummocky moraines, show higher residual doses (22.4–205.6 Gy). Reworked loessic sediments exhibit surprisingly high residual doses (24.1 and 46.5 Gy). Glaciofluvial and materials from lateral moraine (upper part) are recommended when sampling, whereas those from subglacial tills, terminal moraines, ground moraines and hummocky moraines should be avoided.

© 2014 Elsevier Ltd and INQUA. All rights reserved.

1. Introduction

The abundant mountain glacial landforms and the associated sediments in the Qinghai-Tibetan Plateau and the bordering mountains (including the Tianshan Mountains) are valuable archives for reconstructing the glacial history. However, our knowledge about Quaternary glaciations in this region is still limited due to insufficient chronological data. Over the last two decades, optically stimulated luminescence (OSL) methods have been extensively tried for dating glacial sediments in this region (Sharma and Owen, 1996; Owen et al., 1997; Richards, 2000; Richards et al., 2000a, 2000b; Tsukamoto et al., 2002; Xu et al., 2009; Zhao et al., 2009, 2012; B. Zhang et al., 2012; W. Zhang et al., 2012; Wang et al., 2013; Zhao et al., 2013; Hu et al., 2014). However, relatively few studies focused on assessing the adequacy of the methodology (Rhodes and Pownall, 1994; Rhodes and Bailey, 1997; Rhodes, 2000; Richards, 2000; Tsukamoto et al., 2002; Spencer and Owen, 2004; Ou et al., 2010).

It was reported that some of the glacier-related sediments were well bleached, such as glacio-aqueous (glaciofluvial and glaciolacustrine) (Richards, 2000; Alexanderson and Murray, 2007; Boe et al., 2007; Fuchs and Owen, 2008; Alexanderson and Murray, 2012b; King et al., 2014; Ou et al., 2014) and glacio-aeolian deposits (Richards, 2000; Fuchs and Owen, 2008). It was also reported that some glacial sediments were also well bleached, such as supraglacial tills (Richards, 2000; Tsukamoto et al., 2002; Ou et al., 2014) and subglacial sediments (Swift et al., 2010; Bateman et al., 2012). However, incomplete bleaching of glacial sediment still remains one of the most significant problems in luminescence dating (Richards, 2000; Tsukamoto et al., 2002; Spencer and Owen, 2004; Klasen et al., 2007; Lukas et al., 2007; Duller, 2008; Fuchs and Owen, 2008; Thrasher et al., 2009; Alexanderson and Murray, 2012b) and leads to overestimation of age. This has hindered the

* Corresponding author.
** Corresponding author. State Key Laboratory of Cryospheric Sciences, Cold and Arid Regions Environmental and Engineering Research Institute, Chinese Academy of Sciences, Lanzhou, 730000, China.
E-mail addresses: ouxianjiao@163.com (X. Ou), zplai@isl.ac.cn (Z. Lai).

http://dx.doi.org/10.1016/j.quaint.2014.08.053
1040-6182/© 2014 Elsevier Ltd and INQUA. All rights reserved.

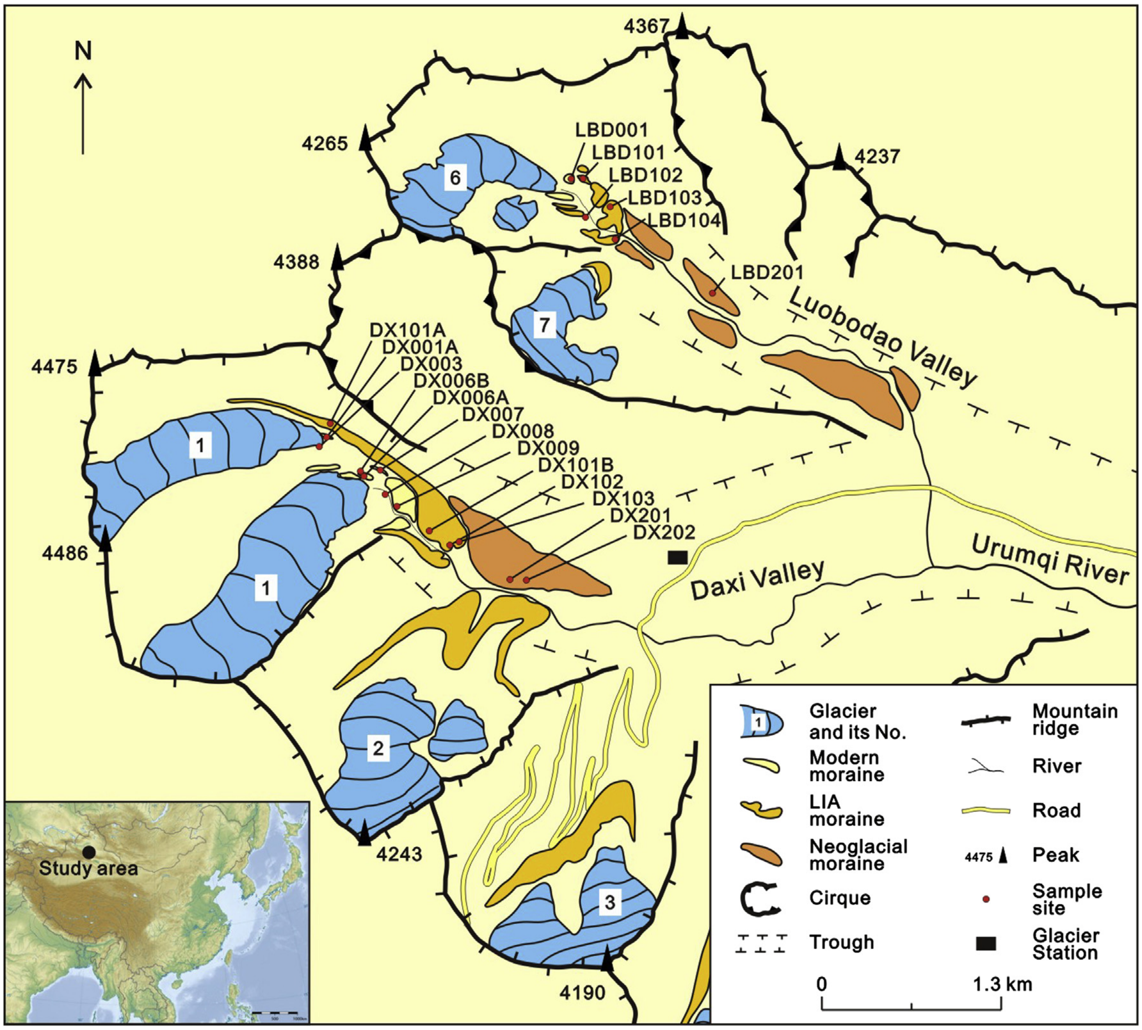

Fig. 1. Young glacial landforms in the source area of the Urumqi River and sampling sites. Samples were collected in the Daxi Valley (DX, thirteen samples) and the Luobodao Valley (LBD, six samples).

application of OSL dating on glacial sediments. Therefore, it is important to assess the incomplete bleaching effect in different glacial depositional environments. Dating young, especially modern analogue sediments, is a good way to test the signal resetting prior to deposition (Duller, 2008; Alexanderson and Murray, 2012a).

The source area of the Urumqi River is a critical place for Quaternary glaciation research in China because the glacial landforms in this area are well preserved and have been dated by multiple techniques including ^{14}C (Zheng and Zhang, 1983; Yi et al., 1998, 2004), lichenometry (Chen, 1989; Wang, 1991), electron spin resonance (ESR) (Yi et al., 2002; Zhou et al., 2002, 2006; Zhao et al., 2006), and terrestrial cosmogenic nuclides (TCN) (Kong et al., 2009; Y. Li et al., 2011). More importantly, young glacial sediments in this area have been dated by conventional ^{14}C (Zheng and Zhang, 1983), AMS ^{14}C (Yi et al., 1998, 2004), and lichenometry (Chen, 1989; Wang, 1991). Therefore, it is an ideal place to test the zero assumption of OSL dating. In this study, nineteen young glacial sediments were sampled as analogues of Pleistocene deposits. Due to dim signal, samples had to be dated using large aliquot quartz OSL methods. The aim of this study is to investigate the bleachability of OSL signal of glacial sediments from different depositional settings and different geomorphological positions. The implications for Quaternary glacial sediment dating are also discussed.

2. Regional setting and samples

The source area of the Urumqi River is located on the northern slope of Kalawucheng Mountain, a part of central Tianshan Mountains, in the Xinjiang Uygur Autonomous Region of China (Fig. 1). This part of the Tianshan Mountains is surrounded by vast deserts: the Taklimakan Desert in the Tarim Basin to the south, the Gurbantunggut Desert in the Junggar Basin to the north, and the Gobi Desert to the east. The westerly jet stream prevails across these high mountains throughout a year (Li et al., 2006).

The highest peak in this area, Tiangeer Peak II, is 4486 m asl. The modern glaciers are mostly cirque glaciers and hanging glaciers and small valley glaciers are also common. Five sets of glacial moraines are distributed along the valley downstream from the modern glaciers (Xu et al., 2010a, 2010b). The samples examined in this paper were young (since the Neoglacial) glacial sediments collected in the frontal of the Glacier No. 1 (43°07′N, 86°49′E) and Glacier No. 6 (43°08′N, 86°50′E).

Glacier No. 1 is a northeast-facing valley glacier, located in the head of the Daxi Valley (Fig. 1; Fig. 2). It has been monitored for more than 40 years (longest in China, since 1958 with interruptions during 1967–1979) and is among those glaciers listed as actively receding by the World Glacier Monitoring Service (Takeuchi and Li, 2008). It is now composed of east and west branches covering

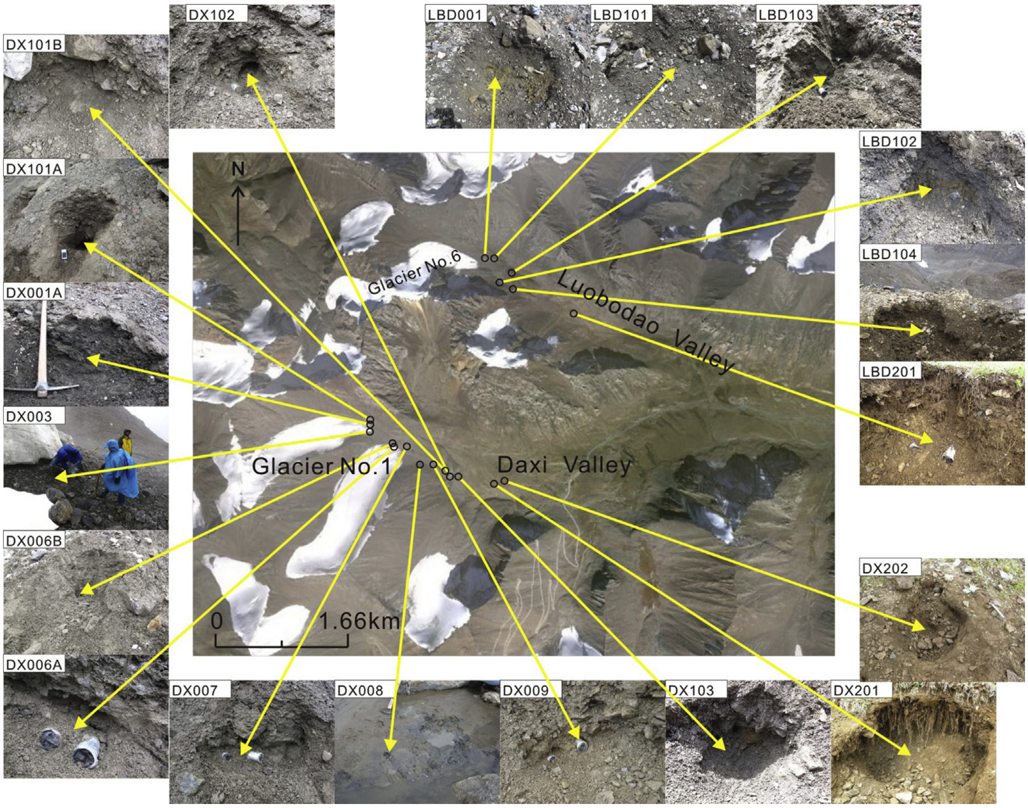

Fig. 2. Google map of the source area of the Urumqi River and sampling sections. The scope of this map is similar to Fig. 1. Photos of sampling sections are showed around the map.

~1.70 km^2 with a length of ~2.20 km. These two branches were separated into two small independent glaciers in 1993 due to persistent glacier shrinkage. The terminus retreated constantly with an average rate of 4.5 m a^{-1} during 1959–1993. After that, the terminuses of east and west branch retreated respectively 6.0 m a^{-1} and 3.5 m a^{-1} during 1994–2008 (Z.Q. Li et al., 2011). The average annual equilibrium line altitude (ELA) is approximately 4055 m a.s.l. during the past 50 years (Z.Q. Li et al., 2011). The annual precipitation is approximately 646 mm at the ELA (Z.Q. Li et al., 2011). The Glacier No.1 now terminates at an altitude of ~3770 m a.s.l. (east branch) and ~3860 m a.s.l. (west branch). The meteorological data have been collected from 1958 to 2003 at the Daxigou Glacier Station located at 3539 m a.s.l., about 3 km downstream of the glacier (Fig. 1). The mean annual temperature and precipitation are −5.1 °C, and 450 mm, respectively (Ye et al., 2005). Glacier No. 6 is also a northeast-facing small valley glacier with an area of about 0.88 km^2 and 1.30 km in length (Zheng and Zhang, 1983) (Fig. 1; Fig. 2). It is located in the head of the Luobodao Valley, adjacent to the Daxi Valley where Glacier No. 1 is situated. The glacier currently terminates at an altitude of ~3790 m.

Glaciers in the source area of the Urumqi River have persistently receded since the Neoglacial and the recessions formed several well-preserved moraines in the valleys (Fig. 1; Fig. 2) (Shi, 2006). In the Daxi Valley, modern moraines are distributed approximately within 400 m in front of the glaciers. Boulders on these moraines do not have any signs of being weathered and no soil or vegetation has developed on the moraines. The outermost modern terminal moraine was formed during the 1960s (Zheng and Zhang, 1983). Beyond these outermost moraines, there are two groups of young moraines: one was formed during the Little Ice Age (LIA) and the other during Neoglaical. In the Daxi Valley, the first group (LIA moraine) includes three lateral-terminal moraines within a distance less than 800 m beyond the snout of the modern glacier. These LIA three moraines are characterized by sharp-crests, fresh-looking boulders, non-pedogenic sign, and sparseness of vegetation coverage. Ages have been obtained for these moraines. There are three lichenometric ages of 1538 ± 20, 1777 ± 20, and 1871 ± 20 AD (Chen, 1989; Wang, 1991), and two AMS ^{14}C ages of 428 ± 127 and 416 ± 146 cal BP obtained from calcium carbonate in tills (Yi et al., 2004).

The second group (Neoglacial moraines) distributes within a distance less than 2 km from the terminal of the glacier. The moraine surfaces are rounded, the boulders on the surfaces are weakly weathered, and the surfaces were covered by thin layer of soil and meadow. The ^{14}C ages for these moraines are 4.4 ± 0.2 cal ka BP (obtained from carbonate coating on till clast) (Zheng and Zhang, 1983), 6.5 ± 0.1 and 4.6 ± 0.2 cal ka BP (obtained from tills) (Chen, 1989), 7.5 ± 0.1 and 1.8 ± 0.1 cal ka BP (obtained from carbonate coating on till clast) (Yi et al., 2004). In the Luobodao Valley, there was no numerical age for any moraines. However, according to the geomorphological characteristics, the moraines in the Luobodao Valley were identified to be similar to those of LIA and Neoglacial moraines in the Daxi Valley (Shi, 2006). According to field investigations and chronological data, Shi (2006) concluded that the Neoglacial advance mainly occurred at 3–4 ka and the LIA glacial advance during 15–19th centuries.

Thirteen samples were collected from glacial sediments in the Daxi Valley beyond the Glacier No. 1 (Fig. 1; Fig. 2). Sample DX001A is from the inside side of a modern ground moraine, only ~10 m from the snout of the west branch of the glacier. Sample DX003 was from modern subglacial tills just beneath the snout of the glacier. Sample DX006A was taken from a glaciofluvial lens in the proximal flank of a modern ground moraine to the left of the east branch of the Glacier No. 1, and sample DX006B is from the outside side of the same moraine. Sample DX007 was from a modern lateral moraine ~110 m to the snout of the east branch. Sample DX008 was from a glaciofluvial bar, ~150 m beyond the snout of the east branch. Sample DX009 was from the 1960s terminal moraine ~220 m beyond the snout of the east branch. Sample DX101A was from the lateral part of the youngest LIA moraine ~80 m to the left of the west branch. Sample DX101B, DX102, and DX103 were collected from the top of the terminal part of the three LIA lateral-terminal moraines, respectively. The sample sites are respectively ~440 m, ~640 m and ~680 m beyond the snout of the east branch. Sample DX201 and DX202 were taken from the Neoglacial terminal moraines, ~1.1 km and ~1.3 km respectively downstream from the glacier. Two glaciofluvial samples (DX006A and DX008) are dominated by medium-coarse sands and silts. The others are till samples which are massive matrix supported diamicton mainly composed of angular gravels, sands, and silts.

Six samples were taken from the Luobodao Valley, beyond the Glacier No. 6 (Fig. 1; Fig. 2). Sample LBD001 was taken from the top of a modern hummocky moraine just ~100 m in front of the glacier. Sample LBD101 and LBD103 were taken from the top of two LIA hummocky moraines, ~190 m and ~390 m respectively from the glacier. Sample LBD102 was from a glaciofluvial lens in a LIA lateral moraine ~280 m in front of the glacier. Sample LBD104 was from the outermost LIA terminal moraine, ~520 m from the glacier. Sample LBD201 was taken from the Neoglacial lateral moraine, ~1.3 km downstream from the glacier. Sample LBD001 and LBD103 were collected from the loessic layer interbedded between tills. They are massive diamicton with angular gravels supported by sandy silt matrix, indicating that they had been redistributed. Sample LBD101, LBD104, and LBD201 are all from tills which are massive matrix supported diamicton dominated by angular gravels, sands, and silts. Sample LBD102 was from glaciofluvial sediments mainly consisting of well sorted sands.

3. Methods

3.1. Sample preparation

Most of the samples were collected by driving iron tubes into the sections. Some of the samples were directly sacked into opaque plastic bags under shade cloth, as it is impossible to drive iron tubes into the sections. In the luminescence dating laboratory, the samples were treated with 10% HCl and 30% H_2O_2 to remove carbonates and organics, respectively. The silt-sized fractions (38–63 μm) were extracted by sieving (Lai, 2010). These fractions were then etched for about two weeks with 38% hydrofluorosilicic acid (H_2SiF_6) to remove the feldspar grains, followed by 10% HCl for 30 min to remove any fluoride precipitates. The purity of quartz grains were monitored by the level of infrared stimulated luminescence (IRSL) signals. Samples that showed obvious IRSL signals were retreated with hydrofluorosilicic acid. However, most of the samples from the Daxi Valley except DX101A and DX201 have IR/blue OSL signal ratios beyond 10% (Table 1), even after retreating with hydrofluorosilicic acid. In contrast, most of the samples from the Luobodao Valley except LBD 103 are lower than 10% (Table 1). Samples were mounted on stainless steel discs by silicone oil, with an area of about 6 mm diameter.

3.2. Measurement procedures

Equivalent dose (D_e) was measured by using the combination of single aliquot regenerative-dose (SAR) protocol (Murray and Wintle, 2000) and the standardized growth curve (SGC) method (Roberts and Duller, 2004; Lai, 2006), i.e. SAR-SGC method (Lai and Ou, 2013). The measurements were performed on an automated Risø TL/OSL-DA-20 reader. During the SAR procedure, a test dose (33 or 45 Gy) was used to monitor sensitivity changes. Preheats of 260 °C for 10 s and 220 °C for 10 s were employed prior to OSL stimulation for regenerative dose and test dose, respectively. Stimulation was carried out using blue LEDs ($\lambda = 470 \pm 20$ nm) for 40 s at 130 °C. Ninety percent diode power was used for all samples. The OSL signal was detected by a 9235QA photomultiplier tube through a 7.5 mm thick Hoya U-340 detection filter. For D_e determination, firstly 6 aliquots were measured for each individual sample using SAR protocol. SGC was then constructed for each sample using the SAR data. Eighteen additional aliquots were measured for their natural (L_N) and test dose (T_N) OSL under the same condition of the SAR procedure. The natural OSL signal corrected by test dose (L_N/T_N) was matched in the SGC to obtain a D_e value. The final D_e for age calculation for a sample was the average of all SAR and SGC D_es. The concentrations of U, Th, and K were measured by Neutron Activation Analysis. Water content was estimated according to the laboratory measurement and the precipitation. The alpha efficiency was taken as 0.035 ± 0.001 (Lai et al., 2008).

As it is not possible to completely remove the effects of feldspar contamination for most of the samples from the Daxi Valley, we tried post-IR OSL method to determine the D_e values for four samples (DX007, DX009, DX101B and DX102). The measurement conditions of post-IR OSL protocol are similar to that of the blue OSL SAR protocol. The only difference is an additional 100 s IR stimulation prior to blue OSL stimulation in each regenerative-dose cycle.

4. Results

4.1. OSL characteristics

Most of the samples in the study area exhibit low luminescence sensitivity (normally tens or hundreds counts/Gy for our 6 mm aliquots, integrated over the first 0.64 s; Fig. 3). The OSL signal was quickly bleached to measurement background within about one second, suggesting that the samples are dominated by the fast component. Most of the samples show similar characteristics, except sample LBD001, LBD101 and LBD102, which show a slower decaying. The recycling ratios of samples from the Daxi Valley range from 0.81 to 1.23, with an exceptional sample DX009 that ranges from 0.47 to 0.56. The values are within 0.9–1.1 for all

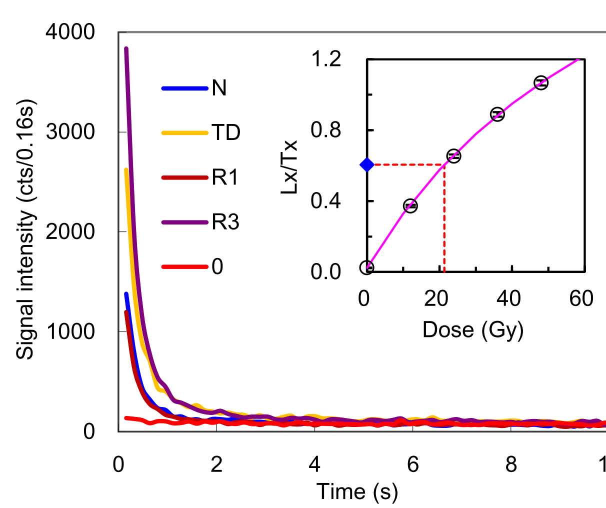

Fig. 3. OSL decay curves of zero dose (0), natural dose (N), test dose (TD, 45 Gy), and regeneration doses (R1 and R3, 12 Gy and 36 Gy, respectively) of sample DX101A. Insert shows growth curve of the sample.

samples from the Luobodao Valley. To test the effect of thermal transfer on the D_e determination, a zero dose cycle was incorporated in the SAR protocol. For the $(L_0/T_0)/(L_N/T_N)$ ratio of the nineteen samples, eight are lower than 5.0%, eight range from 5.2% to 11.1%, and three range from 18.3% to 26.1% (Table 1). Growth curve of sample DX008 is also shown in Fig. 3.

4.2. Preheat plateau and dose recovery

Preheat plateau and dose recovery test could be used to choose a suitable preheat temperature and evaluate the suitability of SAR protocol. In this study, three samples, two from the Daxi Valley (DX008 and DX101A, Figs. 4 (a–c) and (d-f)) and one from the Luobodao Valley (LBD201, Figs. 4 (g–i)), were selected to conduct these tests. For the preheat plateau test, a set of 20 aliquots from each sample were measured by SAR procedure with 5 different preheat temperatures (220–300 °C, four aliquots for each temperature). For sample DX101A (Fig. 4 (e)) and LBD201 (Fig. 4 (h)), no significant difference was found between 220 and 300 °C. For sample DX008 (Fig. 4 (b)), a plateau occurs between 260 and 300 °C while the errors are greater between 220 and 240 °C. Recycling ratios are consistent with unity for preheat temperatures between 260 and 300 °C for sample DX101A (Fig. 4 (f)) and the recuperations rises at temperatures above 280 °C for sample LBD201 (Fig. 4 (i)). The preheat temperature of 260 °C was chosen for the SAR measurement at last.

For dose recovery test, a set of 6 aliquots from each of the three samples were bleached with blue LED for 100 s at room temperature. A laboratory beta dose was then given, followed by SAR measurements. In Fig. 4, the ratios between the measured and given doses are shown. For the samples from the Daxi Valley (DX008 and DX101A, Figs. 4 (a) and (d)), the given dose could not be well recovered. For the sample from the Luobodao Valley (LBD201, Fig. 4 (g)), the given dose was well reproduced. All these data are presented in Fig. 4.

4.3. D_e, apparent ages, residual doses and age overestimations

Most of the SGC D_e values are consistent with SAR D_e values (within 10%) except DX003, DX006A, DX006B, DX009 and DX201. All of the aliquots were included except the abnormal one when calculating the D_e value. Apparent OSL ages with their D_e values and dose rate information are given in Table 1.

As Glacier No. 1 has been monitored since 1958, and the glacial landforms have been dated by numerical methods, the expected ages of the samples in this study can be estimated. The modern samples were determined by geomorphological positions, depositional contexts and the observation records (Zheng and Zhang, 1983; Z.Q. Li et al., 2011). The approximate ages of the LIA and Neoglacial moraine samples were estimated by stratigraphic positions and numerical dates (Zheng and Zhang, 1983; Chen, 1989; Wang, 1991; Yi et al., 2004; Shi, 2006). This allows us to calculate the residual doses and apparent age overestimations (Table 1).

5. Discussion

Almost all of the D_es of the samples in this study were overestimated. Generally speaking, greater residual dose values were obtained for samples from the Daxi Valley than for the sampels from the Luobodao Valley. Only five samples from these two valleys showed relatively low residual doses (<21 Gy) and age overestimations (<4 ka). Two of them (DX008 and LBD102) are glaciofluvial sediments, while the other three (DX007, DX101A and LBD201) are tills from the top of lateral moraines. Fourteen of the nineteen samples showed high residual dose (22.4–205.6 Gy) and age overestimation (6.1–29.6 ka). Among these fourteen samples, one (DX006A) is glaciofluvial sediments (residual dose of 99.8 Gy, age overestimation of 20.6 ka), two of them (LBD001 and LBD103) are loessic sediments (residual dose of 24.1 and 46.5 Gy, age overestimation of 7.7 and 10.4 ka, respectively). The rest are tills from terminal moraines, ground moraines and hummocky moraines, as well as a modern subglacial till samples.

Most of the samples from the Daxi Valley suffer from feldspar contamination, as can be seen from the IR/blue OSL ratios in Table 1. We did not reject aliquots with the 10% criterion because most of aliquots from this valley would be rejected if the criterion is employed, and there is no significant connection between feldspar contamination and residual dose. It is unlikely that feldspar contamination represents a significant contribution to D_e overestimation.

Studies on young glaciofluvial sediments in Himalaya indicated that the thermal transfer occurred during preheating is responsible for large D_e values of glacial sediments (Rhodes and Pownall, 1994; Rhodes and Bailey, 1997; Rhodes, 2000). However, some lower thermal transfer values of young glacial sediments were also reported in this region (B. Zhang et al., 2012; Ou et al., 2014). According to our recuperation test for all of the samples, the thermal transfer values range from 1.7% to 26.1%, with contributions on D_e values ranging from 0.4 to 10.4 Gy (average value 3.5 Gy) (Table 1). It can be seen that thermal transfer is too small to account for the dose overestimation for samples from this area. Furthermore, it is normal for young samples with lower dose to exhibit higher recuperation values, as recuperation is calculated as a percentage of the luminescence signals of the zero dose to the natural dose. All of the three samples which are extremely high in recuperation values have very low natural doses (D_e values). Therefore, thermal transfer is not the reason of overestimation. Partial bleaching is primarily responsible for high dose residual in this study.

The residual dose (partial bleaching) variation in this study seems more likely related to the difference of geomorphological positions and sediment types (Fig. 5). Glacial debris is transported on top of (supraglacial), beneath (subglacial), or within (englacial) a glacier, and released as meltout tills, flow tills, lodgement tills, deformation tills, or sublimation tills, to form different kinds of glacial landforms, such as terminal moraine, lateral moraine, ground moraines, lodgment moraines, or hummocky moraine. The

Table 1
Sample information and luminescence data.

Sample no.	Depth (m)	K (%)	Th (ppm)	U (%)	Water content (%)	Dose rate (Gy/ka)	n^a	SAR D_e (Gy)	SGC D_e (Gy)	SAR D_e/SGC D_e	Method
DX001A	0.50	2.84 ± 0.07	13.75 ± 0.34	4.77 ± 0.17	10 ± 5	5.18 ± 0.35	22/24	30.2 ± 3.2	32.8 ± 2.6	0.92	Blue OSL
DX003	0.20	3.19 ± 0.08	21.16 ± 0.49	8.15 ± 0.24	10 ± 5	6.96 ± 0.48	22/24	226.5 ± 23.5	184.7 ± 5.1	1.23	Blue OSL
DX006A	1.50	2.78 ± 0.08	14.58 ± 0.35	3.72 ± 0.16	10 ± 5	4.85 ± 0.33	21/24	95.1 ± 15.3	104.6 ± 15.3	0.91	Blue OSL
DX006B	0.90	3.29 ± 0.09	18.81 ± 0.43	6.20 ± 0.22	10 ± 5	6.30 ± 0.43	19/22	114.8 ± 4.6	102.5 ± 4.8	1.12	Blue OSL
DX007	0.50	3.44 ± 0.09	21.95 ± 0.50	8.36 ± 0.25	10 ± 5	7.25 ± 0.49	24/24	9.3 ± 1.4	9.6 ± 0.8	0.98	Post-IR
DX008	0.13	2.93 ± 0.08	15.04 ± 0.36	5.99 ± 0.20	10 ± 5	5.70 ± 0.42	22/24	11.6 ± 1.1	11.7 ± 0.8	0.99	Blue OSL

Table 1 (*continued*)

Sample no.	Depth (m)	K (%)	Th (ppm)	U (%)	Water content (%)	Dose rate (Gy/ka)	n^a	SAR D_e (Gy)	SGC D_e (Gy)	SAR D_e/SGC D_e	Method
DX009	2.00	2.84 ± 0.08	18.67 ± 0.43	9.45 ± 0.26	10 ± 5	6.68 ± 0.45	19/22	71.5 ± 10.9	86.4 ± 10.3	0.83	Post-IR
DX101A	0.80	3.10 ± 0.09	15.00 ± 0.36	5.19 ± 0.19	10 ± 5	5.60 ± 0.38	23/24	21.3 ± 1.9	21.3 ± 1.1	1.00	Blue OSL
DX101B	1.00	2.95 ± 0.09	16.66 ± 0.40	5.15 ± 0.21	10 ± 5	5.55 ± 0.38	22/24	79.7 ± 10.3	81.2 ± 7.6	0.98	Post-IR
DX102	0.80	2.74 ± 0.08	14.46 ± 0.35	4.78 ± 0.18	10 ± 5	5.12 ± 0.35	23/24	52.9 ± 8.0	51.7 ± 3.6	1.02	Post-IR
DX103	0.60	3.62 ± 0.10	21.71 ± 0.48	7.59 ± 0.22	10 ± 5	7.18 ± 0.49	20/22	164.0 ± 12.8	173.3 ± 11.7	0.95	Blue OSL
DX201	0.90	2.38 ± 0.07	12.94 ± 0.31	3.31 ± 0.16	10 ± 5	4.29 ± 0.29	24/24	149.1 ± 8.2	125.0 ± 5.8	1.19	Blue OSL
DX202	0.30	1.70 ± 0.07	13.72 ± 0.34	2.99 ± 0.16	10 ± 5	3.71 ± 0.26	23/23	105.8 ± 7.8	111.2 ± 5.1	0.95	Blue OSL
LBD001	0.50	1.35 ± 0.06	9.69 ± 0.29	3.23 ± 0.22	10 ± 5	3.15 ± 0.21	20/20	24.8 ± 1.4	23.6 ± 0.9	1.05	Blue OSL
LBD101	0.50	1.28 ± 0.05	7.63 ± 0.25	1.77 ± 0.20	10 ± 5	2.55 ± 0.18	21/22	69.4 ± 2.4	67.8 ± 2.0	1.02	Blue OSL
LBD102	2.00	1.68 ± 0.06	10.50 ± 0.29	3.05 ± 0.22	10 ± 5	3.36 ± 0.23	24/24	5.4 ± 0.6	5.0 ± 0.3	1.07	Blue OSL
LBD103	0.35	2.25 ± 0.08	15.25 ± 0.40	3.67 ± 0.23	10 ± 5	4.48 ± 0.31	24/24	49.8 ± 2.1	45.2 ± 1.7	1.10	Blue OSL
LBD104	0.40	1.04 ± 0.05	4.94 ± 0.20	1.25 ± 0.20	10 ± 5	2.01 ± 0.15	23/24	23.9 ± 2.4	22.9 ± 0.8	1.04	Blue OSL
LBD201	0.40	2.28 ± 0.08	15.10 ± 0.39	4.14 ± 0.25	10 ± 5	4.62 ± 0.32	24/24	7.4 ± 1.0	8.2 ± 0.5	0.91	Blue OSL

Sample no.	Description	Location	Expected age	D_e (Gy)	Apparent age (ka)	Residual dose (Gy)	IR/OSL	Thermal transfer (%)	Thermal transfer (Gy)
DX001A	Till	Ground moraine	Modern	31.5 ± 2.1	6.1 ± 0.6	31.5	0.22	6.6	2.1
DX003	Till	Subglacial till beneath glacier snout	Modern	205.6 ± 7.3	29.6 ± 2.3	205.6	0.32	3.0	6.2
DX006A	Glaciofluvial	Glaciofluvial lens in ground moraine	Modern	99.9 ± 11.1	20.6 ± 2.7	99.8	0.25	9.7	9.7
DX006B	Till	Ground moraine	Modern	108.7 ± 4.1	17.2 ± 1.3	108.6	0.17	5.9	6.4
DX007	Till	Lateral moraine	Modern	9.4 ± 0.7	1.3 ± 0.1	9.2	0.20	26.1	2.5
DX008	Glaciofluvial	Glaciofluvial bar	Modern	11.6 ± 0.7	2.0 ± 0.2	11.5	0.20	21.3	2.5
DX009	Till	Terminal moraine	Modern (1960s)	79.0 ± 7.8	11.8 ± 1.4	78.6	0.25	4.1	3.2
DX101A	Till	Lateral moraine	LIA (1871 AD?)	21.3 ± 0.9	3.8 ± 0.3	20.5	0.07	3.4	0.7
DX101B	Till	Terminal moraine	LIA (1871 AD)	80.5 ± 6.1	14.5 ± 1.5	79.7	0.30	3.7	3.0
DX102	Till	Terminal moraine	LIA (1777 AD)	52.3 ± 3.3	10.2 ± 0.9	51.1	0.55	10.2	5.3
DX103	Till	Terminal moraine	LIA (1538 AD)	168.7 ± 8.9	23.5 ± 2.0	165.3	0.19	5.2	8.8
DX201	Till	Terminal moraine	Neoglacial (≤4000 yrs)	137.0 ± 5.2	31.9 ± 2.5	~120	0.10	1.7	2.4
DX202	Till	Terminal moraine	Neoglacial (≤4000 yrs)	108.5 ± 4.2	29.3 ± 2.3	~95	0.11	3.7	4.0
LBD001	Loessic sediments	Hummocky moraine	Modern	24.2 ± 0.8	7.7 ± 0.6	24.1	0.04	11.1	2.7
LBD101	Till	Hummocky moraine	LIA (1871 AD?)	68.6 ± 1.5	26.9 ± 1.9	68.2	0.07	18.3	3.6
LBD102	Glaciofluvial	Glaciofluvial lens in lateral moraine	LIA (1777 AD?)	5.2 ± 0.3	1.6 ± 0.1	4.4	0.05	5.3	1.0
LBD103	Loessic sediments	Hummocky moraine	LIA (1777 AD?)	47.5 ± 1.5	10.6 ± 0.8	46.5	0.11	1.8	0.8
LBD104	Till	Terminal moraine	LIA (1538 AD?)	23.4 ± 0.9	11.6 ± 1.0	22.4	0.06	2.0	0.5
LBD201	Till	Lateral moraine	Neoglacial (≤4000 yrs)	7.8 ± 0.4	1.7 ± 0.1	0	0.06	5.2	0.4

[a] Numbers of measured aliquot and accepted aliquot.

finer-grained materials are released and transported by melt water, and deposited as glaciofluvial or glaciolacustrine sediments. Some finer-grained materials are blown by wind and deposited as proglacial sands, loess, or loess-like sediments. The greatest chance of sufficient bleaching of glacial sediments is likely to occur in glaciofluvial, glaciolacustrine and glacioaeolian deposits (Richards, 2000; Fuchs and Owen, 2008). Although poor bleaching of glacial sediments have been reported by many researchers (Richards, 2000; Spencer and Owen, 2004; Klasen et al., 2007; Lukas et al., 2007; Duller, 2008; Thrasher et al., 2009), some studies showed that young glaciofluvial deposits could be well bleached (Alexanderson, 2007; Alexanderson and Murray, 2007; Boe et al., 2007; Ou et al., 2014). Tills may be incompletely bleached owing to shorter daylight exposure during transport and deposition (Tsukamoto et al., 2002; Duller, 2006; Fuchs and Owen, 2008). But supraglacial tills possess a high chance to be sufficiently reset because they are transported on the surface of glacier (Richards, 2000; Tsukamoto et al., 2002; Ou et al., 2014). In contrast, basal tills such as deformation tills and subglacial meltout tills are unlikely to get sufficient exposure (Richards, 2000; Tsukamoto et al., 2002). However, recent studies showed that OSL signal of subglacial sediment might be reset due to subglacial shearing or grinding (Swift et al., 2010; Bateman et al., 2012). Investigation in the Daxi Valley showed that subglacial crushing and abrasion could result in the resetting of ESR signal of Ge centers in quartz sands (Yi et al., 2002).

Glaciofluvial samples in the study area are relatively well reset with an exception. Two (DX008 and LBD102) show low residual doses (11.5 and 4.4 Gy). These doses are small for such a short transport distance. It proves again that glaciofluvial sediments could be well bleached (Richards, 2000; Alexanderson, 2007; Alexanderson and Murray, 2007; Boe et al., 2007; Fuchs and Owen, 2008; Ou et al., 2014). Glaciofluvial lens bedding in moraine is probably considered as an ideal site for OSL sampling, because of its bleachability and a direct link to a specific moraine, which, is considered as a certain indicator of glacial event. However, the sample DX006A from a glaciofluvial lens embedded in a ground moraine shows a surprisingly high residual dose (99.8 Gy). This suggests that glaciofluvial material is not always well bleached. They could have been deposited in subglacial, englacial and supraglacial environments. Furthermore, the existing glaciofluvial sediments could be reworked by glacier re-advance and entrained into a moraine. These sediments might have little chance to exposure to sunlight during transporting and depositing.

The loessic samples (LBD001 and LBD103) in this study show relatively high residual doses (24.1 and 46.5 Gy). They are lower than the samples from subglacial tills, terminal moraines and ground moraines. However, these redistributed loessic samples show quite large doses compared to the original glacio-aeolian deposits, the latter being supposed to be well-bleached (Richards, 2000; Fuchs and Owen, 2008). We assume that these samples might be well bleached during their original deposition. But they

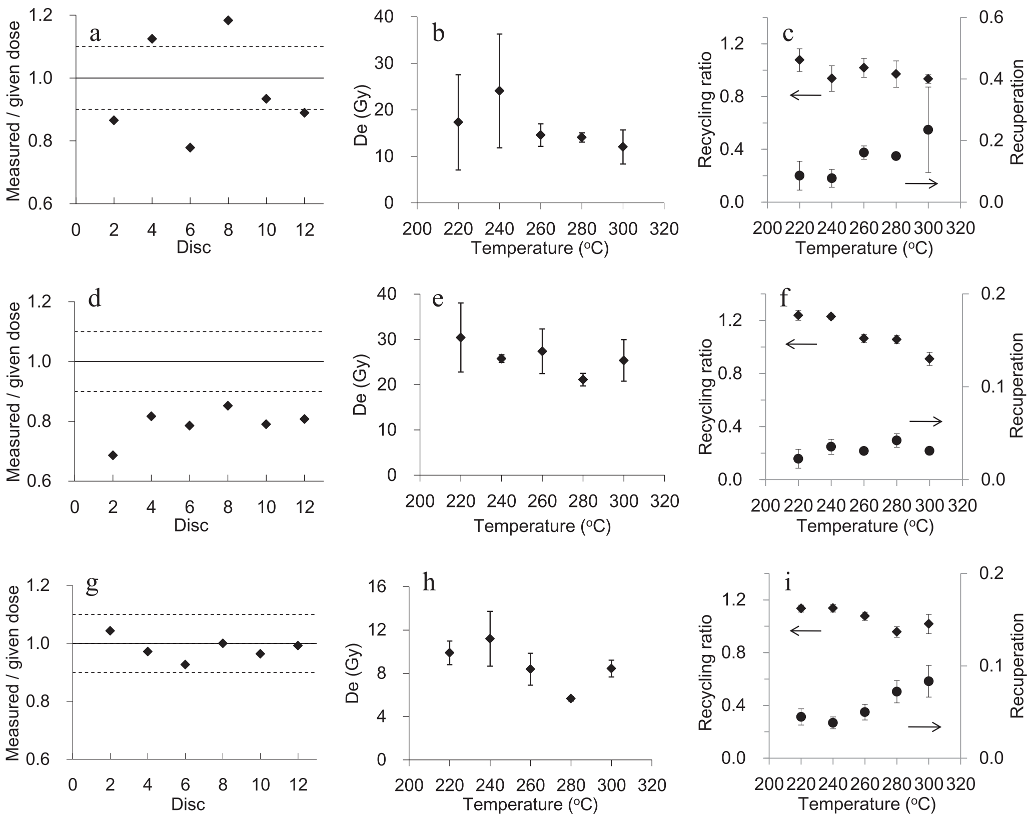

Fig. 4. Dose recovery, preheat plateau, recycling ratio, and recuperation of sample DX008 (a–c), DX101A (d–f) and LBD201 (g–i).

had probably been redistributed without sufficient exposure, because they were inside hummocky moraines (will be discussed below). They probably moved integrally, rather than grain-individually as they did during dust transportation. It seems that the ages of these loessic samples do not represent the formation of the moraines, rather indicate the events of their original deposition.

The modern subglacial till sample (DX003) collected beneath the snout of the west branch of Glacier No.1, shows an extremely high residual dose (205.6 Gy), indicating that it was extremely poorly bleached. This differs from the quartz ESR signal in this area, which could be reset by subglacial process (Yi et al., 2002). It is also contradictory to the hypothesis of subglacial resetting of OSL signal (Swift et al., 2010; Bateman et al., 2012).

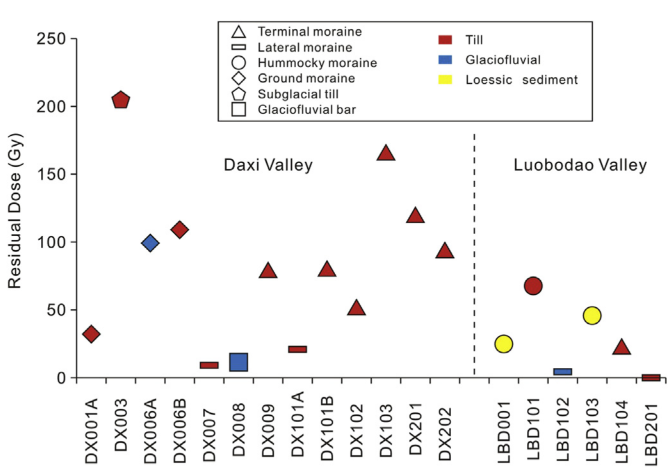

Fig. 5. Relationship between residual doses, geomorphological positions, and depositional settings.

Till samples from terminal moraines (DX009, DX101B, DX102, DX103, DX201, DX202 and LBD104), ground moraines (DX001A and DX006B), and hummocky moraines (LBD101) show high residual doses (22.4–165.3 Gy). For these kinds of moraines, the source of the debris is more complicated. They are probably made up of mixture deposits, including subglacial, englacial, and supraglacial sediments. For ground moraines and hummocky moraines in the study area, they were formed during glacier retreating. All kinds of debris will be dumped to form such kinds of moraines, thus are consisted of various kinds of debris (supraglacial, englacial, and subglacial). The englacial and subglacial debris raises the risk of age overestimation for these moraines. Glaciofluvial (DX006A) and loessic samples (LBD001 and LBD103) inside these moraines show high residual doses. For terminal moraine, it could consist of the previously existing sediments in the glaciated valley, which could be entrained and carried downstream during glacier advances. This also raises the risk of age overestimation.

Samples from lateral moraines (DX007, DX101A and LBD201) show relatively low residual doses (9.2, 20.5 and 0 Gy). We speculate that lateral moraine, especially the upper part of lateral moraine, should be dominated by supraglacial sediments, which are supposed to have more chance to be bleached prior to deposition (Richards, 2000; Tsukamoto et al., 2002; Ou et al., 2014). In the Yingpu Valley of the eastern Qinghai-Tibetan Plateau, young glaciofluvial and lateral moraine samples showed very low residual doses, while low terminal moraine and ground moraine samples exhibit very high residual doses (Ou et al., 2014). The results in this study are similar to those obtained from the Yingpu Valley. However, the small residual doses of the lateral moraine samples show that they might not be completely bleached. It seems that not all of the supraglacial grains have the chance to be exposed to sunlight, although they are transported on the surface of the ice, probably depending on the thickness, the transport and deposit route of the supraglacial debris. If a thick layer of debris is transported and deposited as aggregates, some of the grains might have lost the chance to a complete bleaching.

6. Concluding remarks

In the source area of the Urumqi River, most of the D_es of the young glacial sediments were overestimated when using large aliquot quartz OSL method and the short transport distance might be the blame. The large aliquots may have averaged variously-bleached grains and thus, it is impossible to distinguish incomplete bleaching grains.

Low residual doses were obtained for young glaciofluvial (11.5 and 4.4 Gy) and lateral moraine (0–20.5 Gy) samples, even though they were shortly transported before deposition. Samples from subglacial tills, terminal moraines, ground moraines (including the interbedded glaciofluvial lens), and hummocky moraines show high residual doses (22.4–205.6 Gy). The reworked loessic samples in this study show surprisingly high residual doses (24.1 and 46.5 Gy) compared to the original glacioaeolian deposits that are supposed to be well-bleached. Sediments from terminal moraines, ground moraines and hummocky moraines should be avoided, while glaicofluvial and lateral moraine (upper part) sediments are recommended for OSL dating.

Glacial environment is particularly complicated for OSL dating. Even glaciofluvial and lateral moraine materials are not one hundred percent safe. Careful geomorphological and sedimentological investigation is required before sampling. The OSL applicability varies from place to place. Luminescence characteristics are obviously different even between the neighboring two valleys in the study area. Specific origins and mechanisms of these differences are still difficult to nail down. However, it is apparent that apart from the geomorphological positions and sediment types, the degree of resetting of the OSL signal of glacial sediments might also depend on many other factors and those factors may include the types of bedrock, length of glacier, topography, transport distance, depositional processes, and probably others. The need is thus pressing to conduct more researches for understanding the bleaching mechanisms of glacial sediments and for assessing the applicability of OSL methodology to glacial sediments.

Acknowledgements

We thank DongFeng Niu, JiangLong Wang and WenBin Wang for help in the field. This study is supported by the National Natural Sciences Foundation of China (grants 41371080, 40901011, 41290252 and 41171014) and SKLCS (SKLCS-ZZ-2013-01-05). Zhaodong Feng is gratefully acknowledged for his constructive review that greatly improved the manuscript. Thanks also go to two anonymous reviewers for providing helpful comments.

References

Alexanderson, H., 2007. Residual OSL signals from modern Greenlandic river sediments. Geochronometria 26, 1–9.
Alexanderson, H., Murray, A.S., 2007. Was southern Sweden ice free at 19–25 ka, or were the post LGM glacifluvial sediments incompletely bleached? Quaternary Geochronology 2 (1–4), 229–236.
Alexanderson, H., Murray, A.S., 2012a. Luminescence signals from modern sediments in a glaciated bay, NW Svalbard. Quaternary Geochronology 10, 250–256.
Alexanderson, H., Murray, A.S., 2012b. Problems and potential of OSL dating Weichselian and Holocene sediments in Sweden. Quaternary Science Reviews 44, 37–50.
Bateman, M.D., Swift, D.A., Piotrowski, J.A., Sanderson, D.C.W., 2012. Investigating the effects of glacial shearing of sediment on luminescence. Quaternary Geochronology 10, 230–236.
Boe, A.G., Murray, A., Dahl, S.O., 2007. Resetting of sediments mobilised by the LGM ice-sheet in southern Norway. Quaternary Geochronology 2 (1–4), 222–228.
Chen, J.Y., 1989. Preliminary researches on lichenometric chronology of Holocene glacial fluctuations and on other topics in the headwater of Urumqi River, Tian-Shan Mountains. Science in China (Series B) 32 (12), 1487–1500.
Duller, G.A.T., 2006. Single grain optical dating of glacigenic deposits. Quaternary Geochronology 1 (4), 296–304.
Duller, G.A.T., 2008. Single-grain optical dating of Quaternary sediments: why aliquot size matters in luminescence dating. Boreas 37 (4), 589–612.
Fuchs, M., Owen, L.A., 2008. Luminescence dating of glacial and associated sediments: review, recommendations and future directions. Boreas 37 (4), 636–659.
Hu, G., Yi, C.-L., Zhang, J.-F., Liu, J.-H., Jiang, T., Qin, X., 2014. Optically stimulated luminescence dating of a moraine and a terrace in Laohugou valley, western Qilian Shan, northeastern Tibet. Quaternary International 321, 37–49.
King, G.E., Robinson, R.A.J., Finch, A.A., 2014. Towards successful OSL sampling strategies in glacial environments: deciphering the influence of depositional processes on bleaching of modern glacial sediments from Jostedalen, Southern Norway. Quaternary Science Reviews 89, 94–107.
Klasen, N., Fiebig, M., Preusser, F., Reitner, J.M., Radtke, U., 2007. Luminescence dating of proglacial sediments from the Eastern Alps. Quaternary International 164-165, 21–32.
Kong, P., Fink, D., Na, C.G., Huang, F.X., 2009. Late Quaternary glaciation of the Tianshan, Central Asia, using cosmogenic Be-10 surface exposure dating. Quaternary Research 72 (2), 229–233.
Lai, Z.P., 2006. Testing the use of an OSL Standardised Growth Curve (SGC) for D_e determination on quartz from the Chinese Loess Plateau. Radiation Measurements 41 (1), 9–16.
Lai, Z.P., 2010. Chronology and the upper dating limit for loess samples from Luochuan section in the Chinese Loess Plateau using quartz OSL SAR protocol. Journal of Asian Earth Sciences 37 (2), 176–185.
Lai, Z.P., Ou, X.J., 2013. Basic procedures of optically stimulated luminescence (OSL) dating (In Chinese with English abstract). Progress in Geography 32 (5), 683–693.
Lai, Z.P., Zoller, L., Fuchs, M., Bruckner, H., 2008. Alpha efficiency determination for OSL of quartz extracted from Chinese loess. Radiation Measurements 43 (2–6), 767–770.
Li, Y., Liu, G., Kong, P., Harbor, J., Chen, Y., Caffee, M., 2011. Cosmogenic nuclide constraints on glacial chronology in the source area of the Urumqi River, Tian Shan, China. Journal of Quaternary Science 26 (3), 297–304.
Li, Z.Q., Edwards, R., E, M.-T., Wang, F.T., Dong, Z.B., You, X.N., Li, H.L., Li, C.J., Zhu, Y.M., 2006. Seasonal variability of ionic concentrations in surface snow and elution processes in snow-firn packs at the PGPI site on Urumqi glacier No. 1, eastern Tien Shan, China. Annals of Glaciology 43, 250–256.
Li, Z.Q., Li, H.L., Chen, Y.N., 2011. Mechanisms and simulation accelerated shrinkage of Continental glaciers: a case study of Urumqi glacier No.1 in Eastern Tianshan, Central Asia. Journal of Earth Science 22 (4), 423–430.
Lukas, S., Spencer, J.Q.G., Robinson, R.A.J., Benn, D.I., 2007. Problems associated with luminescence dating of Late Quaternary glacial sediments in the NW Scottish Highlands. Quaternary Geochronology 2 (1–4), 243–248.
Murray, A.S., Wintle, A.G., 2000. Luminescence dating of quartz using an improved single-aliquot regenerative-dose protocol. Radiation Measurements 32 (1), 57–73.
Ou, X.J., Lai, Z.P., Zhou, S.Z., Zeng, L.H., 2014. Timing of glacier fluctuations and trigger mechanisms in eastern Qinghai-Tibetan Plateau during the Late Quaternary. Quaternary Research 81 (3), 464–475.
Ou, X.J., Xu, L.B., Lai, Z.P., Long, H., He, Z.L., Fan, Q.S., Zhou, S.Z., 2010. Potential of quartz OSL dating on moraine deposits from eastern Tibetan Plateau using SAR protocol. Quaternary Geochronology 5 (2–3), 257–262.
Owen, L.A., Bailey, R.M., Rhodes, E.J., Mitchell, W.A., Coxon, P., 1997. Style and timing of glaciation in the Lahul Himalaya, northern India: a framework for reconstructing late Quaternary palaeoclimatic change in the western Himalayas. Journal of Quaternary Science 12 (2), 83–109.
Rhodes, E.J., 2000. Observations of thermal transfer OSL signals in glacigenic quartz. Radiation Measurements 32 (5–6), 595–602.
Rhodes, E.J., Bailey, R.M., 1997. The effect of thermal transfer on the zeroing of the luminescence of quartz from recent glaciofluvial sediments. Quaternary Science Reviews 16 (3–5), 291–298.
Rhodes, E.J., Pownall, L., 1994. Zeroing of the OSL signal in quartz from young glaciofluvial sediments. Radiation Measurements 23 (2–3), 581–585.
Richards, B.W.M., 2000. Luminescence dating of Quaternary sediments in the Himalaya and High Asia: a practical guide to its use and limitations for constraining the timing of glaciation. Quaternary International 65-66, 49–61.
Richards, B.W.M., Benn, D.I., Owen, L.A., Rhodes, E.J., Spencer, J.Q., 2000a. Timing of late Quaternary glaciations south of Mount Everest in the Khumbu Himal, Nepal. Geological Society of America Bulletin 112 (10), 1621–1632.
Richards, B.W.M., Owen, L.A., Rhodes, E.J., 2000b. Timing of Late Quaternary glaciations in the Himalayas of northern Pakistan. Journal of Quaternary Science 15 (3), 283–297.
Roberts, H., Duller, G.A.T., 2004. Standardised growth curves for optical dating of sediment using multiple-grain aliquots. Radiation Measurements 38 (2), 241–252.

Sharma, M.C., Owen, L.A., 1996. Quaternary glacial history of NW Garhwal, central Himalayas. Quaternary Science Reviews 15 (4), 335–365.

Shi, Y.F., 2006. Quaternary Glaciations and Environmental Variations in China (in Chinese). Hebei Science and Technology Press, Shijiazhang.

Spencer, J.Q., Owen, L.A., 2004. Optically stimulated luminescence dating of Late Quaternary glaciogenic sediments in the upper Hunza valley: validating the timing of glaciation and assessing dating methods. Quaternary Science Reviews 23 (1–2), 175–191.

Swift, D.A., Sanderson, D.C.W., Nienow, P.W., Bingham, R.G., Cochrane, I.C., 2010. Anomalous luminescence of subglacial sediment at Haut Glacier d'Arolla, Switzerland – a consequence of resetting at the glacier bed? Boreas 40 (3), 446–458.

Takeuchi, N., Li, Z.Q., 2008. Characteristics of surface dust on urumqi glacier No. 1 in the Tien Shan mountains, China. Arctic, Antarctic, and Alpine Research 40 (4), 744–750.

Thrasher, I.M., Mauz, B., Chiverrell, R.C., Lang, A., 2009. Luminescence dating of glaciofluvial deposits: a review. Earth-Science Reviews 97 (1–4), 133–146.

Tsukamoto, S., Asahi, K., Watanabe, T., Rink, W.J., 2002. Timing of past glaciations in Kanchenjunga Himal, Nepal by optically stimulated luminescence dating of tills. Quaternary International 97-98, 57–67.

Wang, J., Pan, B.T., Zhang, G.L., Cui, H., Cao, B., Geng, H.P., 2013. Late Quaternary glacial chronology on the eastern slope of Gongga Mountain, eastern Tibetan Plateau, China. Science China Earth Sciences 56 (3), 354–365.

Wang, Z.T., 1991. The glacier and environment in the middle sector of Tianshan and the eastern sector of Qilianshan since the Little Ice Age (in Chinese with English Abstract). Acta Geographica Sincica 46 (2), 160–168.

Xu, X., Wang, L., Yang, J., 2010a. Last Glacial Maximum climate inferences from integrated reconstruction of glacier equilibrium-line altitude for the head of the Urumqi River, Tianshan Mountains. Quaternary International 218 (1–2), 3–12.

Xu, X., Yang, J., Dong, G., Wang, L., Miller, L., 2009. OSL dating of glacier extent during the Last Glacial and the Kanas Lake basin formation in Kanas River valley, Altai Mountains, China. Geomorphology 112 (3–4), 306–317.

Xu, X.K., Kleidon, A., Miller, L., Wang, S.Q., Wang, L.Q., Dong, G.C., 2010b. Late Quaternary glaciation in the Tianshan and implications for palaeoclimatic change: a review. Boreas 39 (2), 215–232.

Ye, B., Yang, D., Jiao, K., Han, T., Jin, Z., Yang, H., Li, Z., 2005. The Urumqi River source glacier No. 1, Tianshan, China: changes over the past 45 years. Geophysical Research Letters 32 (21), L21504.

Yi, C.L., Jiao, K.Q., Liu, K.X., He, Y.Q., Ye, Y.G., 2002. ESR dating of the sediments of the Last Glaciation at the source area of the Urumqi River, Tian Shan Mountains, China. Quaternary International 97-98, 141–146.

Yi, C.L., Liu, K.X., Cui, Z.J., 1998. AMS dating on glacial tills at the source area of the Urumqi River in the Tianshan Mountains and its implications. Chinese Science Bulletin 43 (20), 1749–1751.

Yi, C.L., Liu, K.X., Cui, Z.J., Jiao, K.Q., Yao, T.D., He, Y.Q., 2004. AMS radiocarbon dating of late Quaternary glacial landforms, source of the Urumqi River, Tien Shan – a pilot study of C-14 dating on inorganic carbon. Quaternary International 121, 99–107.

Zhang, B., Ou, X.J., Lai, Z.P., 2012. OSL ages revealing the glacier retreat in the Dangzi valley in the eastern Tibetan Plateau during the Last Glacial Maximum. Quaternary Geochronology 10, 244–249.

Zhang, W., He, M.Y., Li, Y.H., Cui, Z.J., Wang, Z.L., Yu, Y., 2012. Quaternary glacier development and the relationship between the climate change and tectonic uplift in the Helan Mountain. Chinese Science Bulletin 57 (34), 4491–4504.

Zhao, J.D., Lai, Z.P., Liu, S.Y., Song, Y.G., Li, Z.Q., Yin, X.F., 2012. OSL and ESR dating of glacial deposits and its implications for glacial landform evolution in the Bogeda Peak area, Tianshan range, china. Quaternary Geochronology 10, 237–243.

Zhao, J.D., Liu, S.Y., He, Y.Q., Song, Y.G., 2009. Quaternary glacial chronology of the Ateaoyinake River Valley, Tianshan Mountains, China. Geomorphology 103 (2), 276–284.

Zhao, J.D., Yin, X.F., Harbor, J.M., Lai, Z.P., Liu, S.Y., Li, Z.Q., 2013. Quaternary glacial chronology of the Kanas River valley, Altai Mountains, China. Quaternary International 311, 44–53.

Zhao, J.D., Zhou, S.Z., He, Y.Q., Ye, Y.G., Liu, S.Y., 2006. ESR dating of glacial tills and glaciations in the Urumqi River headwaters, Tianshan Mountains, China. Quaternary International 144, 61–67.

Zheng, B.X., Zhang, Z.S., 1983. Fluctuation of glaciers during Neoglaciation in Bogda and the Urumqi River head, Tian Shan (in Chinese with English abstract). Journal of Glaciology and Geocryology 5 (3), 133–142.

Zhou, S.Z., Jiao, K.Q., Zhao, J.D., Zhang, S.Q., Cui, J.X., Xu, L.B., 2002. Geomorphology of the Urumqi River Valley and the uplift of the Tianshan Mountains in Quaternary. Science in China Series D-Earth Sciences 45 (11), 961–968.

Zhou, S.Z., Wang, X.L., Wang, J., Xu, L.B., 2006. A preliminary study on timing of the oldest Pleistocene glaciation in Qinghai-Tibetan Plateau. Quaternary International 154, 44–51.